SPANDIDOS PUBLICATIONS

The cohesin-interacting protein, precocious dissociation of sisters 5A/sister chromatid cohesion protein 112, is up-regulated in human astrocytic tumors

CARSTEN HAGEMANN[1], BETTINA WEIGELIN[1], STEPHAN SCHOMMER[1], MARKUS SCHULZE[1], NAIF AL-JOMAH[2], JELENA ANACKER[3], STEFANIE GERNGRAS[1], SIGLINDE KÜHNEL[1], ALMUTH F. KESSLER[1], BÜLENT POLAT[4], RALF-INGO ERNESTUS[1], RAJNIKANT PATEL[2] and GILES H. VINCE[1]

[1]Tumorbiology Laboratory, Department of Neurosurgery, University of Würzburg, Josef-Schneider-Str. 11, D-97080 Würzburg, Germany; [2]Department of Biochemistry, Henry Wellcome Building, University of Leicester, Lancaster Road, Leicester LE1 9HN, UK; [3]Department of Obstetrics and Gynaecology, University of Würzburg, Josef-Schneider-Str. 4; [4]Department of Radiation Oncology, University of Würzburg, Josef-Schneider-Str. 11, D-97080 Würzburg, Germany

Received June 21, 2010; Accepted August 26, 2010

DOI: 10.3892/ijmm.2010.551

Abstract. Glioblastoma multiforme (GBM) is the most prevalent, highly malignant, invasive and difficult-to-treat primary brain tumor in adults. At the genetic level, it is characterized by a high degree of chromosomal instability and aneuploidy. It has been shown that defects in the mitotic spindle checkpoint could lead to the development of aneuploidy as well as tumorigenesis. Additional proteins regulating sister chromatid cohesion could also be involved in maintaining the fidelity of chromosome segregation. One such protein is the precocious dissociation of sisters 5A (Pds5A), also known as sister chromatid cohesion protein 112. It is a nuclear protein, expressed from the S right through to the mitotic phase. It is highly conserved from yeast to man and plays a role in the establishment, maintenance and dissolution of sister chromatid cohesion. The mutation of Pds5A orthologs in lower organisms results in chromosome missegregation, aneuploidy and DNA repair defects. It is considered that such defects can cause either cell death or contribute to the development of cancer cells. Indeed, altered expression levels of Pds5A have been observed in tumors of the breast, kidney, oesophagus, stomach, liver and colon. Malignant gliomas, however, have not been analysed so far. Herein, we report on the cloning of *Rattus norvegicus* Pds5A and on the analysis of its expression pattern in rat tissue. We also show that Pds5A is significantly overexpressed at both the mRNA and protein level and that this overexpression correlates positively with the WHO grade of human gliomas. However, functional assays show that the siRNA-mediated knockdown of Pds5A affects sister chromatid cohesion but does not influence mitotic checkpoint function or the proliferation and survival of GBM cells. Although the mechanism by which Pds5A functions in GBM cells remains unclear, its overexpression in high grade gliomas implies that it could play a pivotal role during the development and progression of astrocytic tumors.

Correspondence to: Dr Carsten Hagemann, Tumorbiology Laboratory, Department of Neurosurgery, University of Würzburg, Josef-Schneider-Str. 11, D-97080 Würzburg, Germany
E-mail: hagemann_c@klinik.uni-wuerzburg.de

Key words: astrocytoma, cell cycle, expression analysis, glioblastoma multiforme, glioma, precocious dissociation of sisters 5A, sister chromatid cohesion protein 112, sister chromatid cohesion

Introduction

Chromosomal instability and aneuploidy, the gain and loss of chromosomes, is a characteristic of most malignant cells that is seen during the early stages of tumor development (1,2). It is thought that such alterations lead to the deregulation of the signalling network within the cells with the loss of tumor suppressor genes and the overexpression of oncogenes that drive tumorigenesis (3-7). Usually, the mitotic spindle checkpoint ensures the fidelity of sister chromatid segregation during mitosis by delaying the onset of anaphase until the kinetochores of all the chromosomes have attached to the spindle microtubules (8,9). It has been shown that the expression of spindle checkpoint proteins (e.g. Bub1, BubR1, Mad2A) is altered in human malignancies (8,10-12), and in animal models, such changes lead to an increased susceptibility to tumor induction by chemicals and carcinogens (13,14) or even directly cause cancer development (15,16). A defective spindle checkpoint is also the cause of the human chromosomal instability syndrome, which is characterized by premature chromatid separation and mosaic variegated aneuploidy (17-20). These patients do not only suffer from severe developmental defects, but are also very prone to cancer development (21,22).

The protein precocious dissociation of sisters 5 (Pds5), which is also known as sister chromatid cohesion protein 112 (SCC-112) (Table I), is a nuclear protein expressed from the S right through to the mitotic phase, at the time when sister chromatid cohesion exists (23-26). It is highly conserved from yeast to man (Table I) and interacts with the cohesin protein complex, although it is not a cohesin subunit itself (23,24,27-30). Cohesin forms a ring-like structure and holds sister chromatids together until spindle fibers attach to the kinetochores (9,31-33). Anaphase is initiated by the proteolysis of the cohesin subunit, SCC-1, by an endopeptidase called separase (32,33). Cohesin is dissolved, and the sister chromatids are released and distributed equally between the daughter cells by the mitotic spindle (9,31). Our understanding of the mechanism of sister chromatid cohesion and segregation has largely been derived from experiments on the budding yeast, *Saccharomyces cerevisiae* (32,33). In fission yeast and vertebrate cells, separase plays a less important role in sister chromatid separation and it is thought that other mechanisms could regulate chromatid segregation in these cell types (30). It has been shown that Pds5 could be involved in the establishment, maintenance and dissolution of cohesion in both yeasts and humans (27-30,34,35). It could also be implicated in embryonic development (36). The structure of *S. cerevisiae* Pds5p contains ~26 HEAT repeats suggesting that it could act as a scaffold protein with numerous sites for binding the globular domains of other proteins (27). Nonetheless, the detailed mechanism of its function remains unresolved.

The homologous recombination repair of DNA double strand breaks (DSB) is dependent on sister chromatid cohesion, as the intact sister chromatid paired to the damaged chromatid, serves as the repair template (37) and this DSB-repair is defective if Pds5p is not present during meiosis in *S. cerevisiae* (38). The mutants of BimD and Spo76, the orthologs of Pds5 in *Aspergillus nidulans* and *Sordaria macrospora* respectively, are hypersensitive after exposure to DNA damaging agents (39,40) and in the fission yeast, *Schizosaccharomyces pombe*, Pds5$^+$ is required for both cell survival following DNA damage and for accurate chromosome segregation (41). In human cells, Pds5 is involved in stabilizing replication forks and the disturbance of this mechanism leads to the spontaneous appearance of DNA damage (42,43). Therefore, defects in Pds5 expression not only result in chromosome missegregation and aneuploidy, but also in DNA repair defects and this could cause the death and oncogenesis of mitotic cells. Indeed, the overexpression of the human ortholog of Pds5A in Cos1 and MDA-MB231 breast cancer cells, led to apoptotic cell death as was shown by an increase in the number of cells in the sub-G1 phase and the enhanced activation of caspase-3 (25). In addition, the down-regulation of Pds5A mRNA was observed in both breast and kidney tumor samples when compared to the corresponding normal tissues (25), whereas another study reported the up-regulation of Pds5A mRNA and protein levels in tumors of the oesophagus, stomach, liver and transverse colon (26). The overexpression of Pds5A in 293T cells and 3 nasopharyngeal epithelial cell lines (NP69, CNE-2 and C666-1) led to increased colony formation and a higher growth rate, whereas the expression of Pds5A siRNA had the opposite effect (26). Together, these data suggest that Pds5A could have tissue-specific and bifunctional roles in tumorigenesis, showing either tumor suppressor activity or promoting cell proliferation, depending on the cell- and tissue-type (26).

Currently, there are no data concerning Pds5A expression in human astrocytic tumors that display a high level of aneuploidy during their early stages of development (5,44,45). Diffuse astrocytomas WHO grade II (low grade astrocytomas, LGAs) are well differentiated tumors with diffuse infiltration of the adjacent brain parenchyma (46). Most of these tumors progress to anaplastic astrocytomas WHO grade III or glioblastoma multiforme (GBM) within 4-5 years after diagnosis (47). GBM is the most prevalent, highly malignant, invasive and difficult-to-treat primary brain tumor in adults. The treatment regimen of patients with GBM includes neurosurgical tumor resection followed by local γ-irradiation and chemotherapy (46). However, in spite of multidisciplinary treatment the median survival is 14.6 months (48). Therefore, it is vital to identify new potential therapeutic targets for future small molecule therapies. Targeting factors involved in the regulation of DNA damage response, mitosis and their cell cycle checkpoints could be a good strategy to prevent the progression of LGAs to high grade malignancies. Pds5A could be a candidate for such treatment options.

Here, we report on the cloning of *Rattus norvegicus* Pds5A from pheochromocytoma PC12 cells, the expression pattern of Pds5A in different rat tissues and on the overexpression of Pds5A at both the mRNA and protein level, which correlates with the WHO grade of human gliomas. In addition, we examined the potential role of Pds5A in the mitotic checkpoint, sister chromatid cohesion and the proliferation and survival of GBM cells.

Materials and methods

Cloning of full-length rat Pds5A. Total RNA was extracted from rat pheochromocytoma PC12 cells using the SV total RNA isolation kit (Promega, Mannheim, Germany) and mRNA was enriched with the Oligotex® mRNA mini kit (Qiagen, Hilden, Germany). The RevertAid™ first strand cDNA synthesis kit (Fermentas, St. Leon-Rot, Germany) was used to generate the cDNA. The cDNA for *Rattus norvegicus* Pds5A was cloned by the PCR amplification of 3 overlapping fragments using the primers 5'-CCC GGG ATC CCA GGA TGG ACT TCA CGC A-3' (forward) and 5'-GAT ATC GTT CAT CAG TTT CAC TAG TG-3' (reverse) for the N-terminal fragment 1 (1917 bp), 5'-CAC TAG TGA AAC TGA TGA AC-3' (forward) and 5'-CTC GAG TCT GAT GCC TCT GAA CTC TG-3' (reverse) for the middle part (fragment 2, 1690 bp) and 5'-CCT ACT GGA GTA CTA GGT AC-3' (forward) and 5'-AAT CTC TCG AGG TTT GGC CTT CAT TTT CTC C-3' (reverse) for the C-terminal fragment 3 (633 bp). Thermocycle parameters were as follows: Five minutes at 94˚C, 32 cycles of 30 sec at 94˚C, 30 sec at 56˚C (57˚C for fragment 1), 1 min at 72˚C and 10 min at 72˚C. The amplification products were purified using the Nucleo Spin® Extract II kit (Macherey-Nagel, Düren, Germany) and cloned into the pGEMT®-Easy Vector (Promega) following the manufacturer's instructions. The full-length Pds5A cDNA sequence was determined by extended hotshot sequencing (Seqlab, Göttingen, Germany).

SPANDIDOS PUBLICATIONS

Table I. Comparison of the Pds5 protein in different species.

Species	Name	Alternate names	Accession (protein)	Size (amino acids)	Identity (%)								
					S. cerevisiae	*S. pombe*	*A. nidulans*	*S. macrospora*	*D. melanogaster*	*C. elegans*	*X. laevis*	*R. norvegicus*	*H. sapiens* (Pds5A)
Saccharomyces cerevisiae	Pds5p		NP_013793	1277									
Schizosaccharomyces pombe	Pds5+		BAB71784	1205	25								
Aspergillus nidulans	BimD		AAA03063	1506	24	26							
Sordaria macrospora	Spo76		CAB51808	1596	26	26	43						
Drosophila melanogaster	Pds5		NP_610719	1218	21	20	23	20					
Caenorhabditis elegans	Evl-14		NP_497865	1570	18	17	-	-	20				
Xenopus laevis	Pds5A		AAV84283	1323	18	22	22	20	37	21			
Rattus norvegicus	Pds5A	SCC-112	ABO47655	1333	19	23	23	21	37	20	88		
Homo sapiens	Pds5A	SCC-112	NP_001093869	1337	19	23	23	21	37	20	86	97	
	Pds5B	AS3, APRIN	NP_055847	1447	19	25	21	20	37	21	69	72	73

Protein identities were calculated using the program, BLAST 2 Sequences (www.ncbi.nlm.nih.gov/blast/bl2seq/wblast2.cgi), using standard settings.

Tissue samples. Tumor biopsies were obtained from patients treated at the University Hospital of Würzburg. Informed consent was obtained from the patients for the acquisition of tumor material and the study was approved by the local ethics committee. The GBM patients underwent surgical tumor resection followed by radiotherapy and temozolomide chemotherapy, except for GBM samples 2369 and 2423. These were from recurring tumors pre-treated with γ-irradiation and chemotherapy. The human brain tumors were classified by routine histology based on the WHO criteria (49). Temporal brain tissue samples (normal brain, NB) came from patients with epilepsy (kindly provided by Thomas Freiman, at the University Hospital of Freiburg im Breisgau, Germany). Details about patient gender, age, diagnosis, location of tumor and treatment regimen have been described previously (50). Organs for expression studies were taken from Sprague-Dawley rats (Harlan Winkelmann, Borchen, Germany). Immediately after removal all tissue samples were frozen at -80˚C and then stored in liquid nitrogen.

Cells and cell culture. The human GBM cell lines, U87, U251, U343 and U373, were originally purchased from the American Type Culture Collection (Rockville, MD), and GaMG was established from a patient with GBM (Gade Institute of the University of Bergen, Norway) (51). Cell lines were grown as previously described (52) in 75 cm^2 flasks (Corning, NY) at 37°C in an atmosphere of 5% CO_2 and 100% humidity.

siRNA transfection. Cells were transfected by nucleofection (Lonza, Cologne, Germany) as previously described (52,53). Pds5A specific siRNA 5'-CAGCGAUGUUGGUUAGUG ATT-3' was synthesized by Qiagen. siRNA (2 μM or 750 nM) was used per transfection, as indicated. Transfected cells were transferred to 6-well plates and incubated for 24 h or more, as previoulsy described. For chromosome spreading assays, a SMARTpool of 4 Pds5A oligonucleotides (5'-GAUAAAC GGUGGCGAGUAA-3', 5'-CCAAUAAAGAUGUGCGU CU-3', 5'-GAACAGCAUUGACGACAAA-3' and 5'-GAGA GAAAUAGCCCGGAAA-3') and non-targeting, control siRNA oligonucleotides were purchased from Thermo Scientific (CO, USA). The siRNA oligonucleotides were dissolved in RNase-free buffer (20 mM KCl, 6 mM Hepes, 0.2 mM $MgCl_2$, pH 7.5) at a concentration of 20 μM. Cells were transfected with the siRNA oligonucleotides using Interferin reagent (BioScience Autogen, Nottingham, UK) following the manufacturer's instructions.

RNA and protein extraction. Trypsinised cells were washed twice with phosphate-buffered saline (PBS) and then resuspended in 50 μl PBS. Total mRNA and protein were purified from these cells and from 30 mg of tissue samples by the Nucleo-Spin RNA/Protein Kit (Macherey-Nagel) following the manufacturer's instructions and as previously described (50). Purified RNA samples were stored at -80˚C. Proteins were solubilized in 100 μl protein loading buffer containing 50 mM Tris (2-carboxyethyl) phosphine hydrochloride reducing agent. These mixtures were stored at -20˚C.

Semiquantitative RT-PCR analysis. Semiquantitative RT-PCR was performed as described previously (50). The amount

of cDNA was normalised to the respective expression of the housekeeping gene, ß-actin. Pds5A cDNA amplification and expression analysis was performed using the primers 5'-ATG TCT CGC TTG CGA TTA GC-3' (forward) and 5'-TCA TGG GCT AGC AGG TGA AT-3' (reverse). The primers were designed and PCR was performed as described previously (50,54). Thermocycle parameters were as follows: Five minutes at 94˚C, 32 cycles of 30 sec at 94˚C, 30 sec at 59˚C, 1 min at 72˚C and 10 min at 72˚C. The amplification products were separated on 1% agarose gels containing 0.07 μg/ml ethidium bromide.

Western blotting. The expression of Pds5A protein in the GBM cell lines and human tumor biopsies was determined by Western blotting as described previously (54) using NuPAGE® 3-8% Tris-acetate polyacrylamide gels (Invitrogen, Heidelberg, Germany). Proteins were blotted to a nitrocellulose membrane (Schleicher & Schüll, Dassel, Germany). After blocking in 5% milk powder, the membrane was incubated with rabbit polyclonal anti-SCC-112 antibody (Bethyl Laboratories Inc., Montgomery, TX, USA) and diluted 1:500 in TBST [50 mM Tris Base, 150 mM NaCl, 0.1% (v/v) Tween-20] containing 5% milk powder. Mouse monoclonal anti-γ-tubulin primary antibody (Sigma, Deisenhofen, Germany) was used at a dilution of 1:5000 in TBST. Rabbit polyclonal cleaved caspase-3 antibody (Cell Signaling, Danvers, MA, USA) was used at a dilution of 1:1000. After washing in TBST, the membrane was incubated with horseradish peroxidase (HRP) conjugated secondary antibodies: Goat anti-rabbit IgG HRP (Santa Cruz, CA, USA) or sheep anti-mouse IgG HRP (Amersham Pharmacia Biotech, Braunschweig, Germany), both diluted 1:1000 in TBST. Blots were developed in the darkroom using the ECL-immunodetection system (Amersham Pharmacia Biotech).

Immunohistochemistry. GBM sections (2 μm) were cut from formalin-fixed, paraffin-embedded tissue blocks and stained as previously described (50,54) using the same antibody as mentioned above for Western blotting, except that it was used at a dilution of 1:1000. Pds5A protein expression was visualized using the streptavidin-biotin system (Dako, Hamburg, Germany) and diaminobenzidine (DAB; Sigma) as a substrate, which resulted in brown staining. The slides were counterstained with haematoxylin and analysed using a light microscope BX41 (Olympus, Hamburg, Germany). Negative control experiments were carried out by staining with appropriate isotype control antibodies.

FACS analysis. U251 cells were transfected with 2 μM Pds5A siRNA as described above. The medium was changed 72 h later, and 25 ng/ml nocodazole were added to interfere with spindle formation and the induction of the mitotic checkpoint. After 24-h incubation floating cells from the medium were harvested by centrifugation at 230 x g and adherent cells by trypsinisation. Both cell populations were combined, washed once with PBS and finally resuspended in 500 μl PBS. The cells were then fixed in ethanol and stained with propidium iodide (Sigma). Analysis of the DNA content was performed by flow cytometry (FACScalibur, Becton-Dickinson, Franklin Lakes, NJ, USA).

Proliferation assay. U251 cells ($5x10^5$) were transfected with 750 nM Pds5A siRNA as described above and equally distributed to six 60-mm petri-dishes (Corning), filled with 3 ml medium each. The cells were then harvested at 24, 48, 72, 96, 120 and 144 h by trypsinisation and counted using a Fuchs-Rosenthal chamber. The fold increase in cell number was calculated to establish growth curves.

Apoptosis assay. The U251 and GaMG cells were transfected with 2 μM Pds5A siRNA as described above and incubated for 72 h, before the medium was replaced by medium containing DMSO, 50 μM cisplatin, 100 ng/ml nocodazole or 1 μg/ml staurosporine (all from Sigma). The cells were harvested 24 h later and analysed for the presence of cleaved caspase-3 by Western blotting as described above.

3-(4,5-Dimethylthiazol-2-yl)-2,5-diphenyltetrazolium bromide (MTT) assay. Seventy-two hours after transfection with 1 μM Pds5A siRNA, 8000 U251 cells were plated into each well of a 96-well plate, and treated with control medium, 100 ng/ml nocodazole and 50 μM cisplatin, respectively. The viability of the cells was determined 24 h later using the MTT assay (cell proliferation kit I; Roche, Mannheim, Germany). The absorbance at 570 nm was recorded using the 96-well microplate reader Titertek Multiskan Plus (Titertek, Huntsville, AL, USA).

Chromosome spreads. U251 cells were transfected with either Pds5A siRNA or control siRNA and 48 h post-transfection the cells were treated with either taxol (1 μM for 24 h) or with a mixture of taxol (1 μM) and okadaic acid (1 μM) for 12 h. Chromosome spreads from the U251 cells were then prepared as follows: Cells were harvested by mitotic shake-off and swollen in hypotonic sodium chloride (75 mM) for 25 min at 37˚C. The cells were then centrifuged (1000 rpm for 10 min) and resuspended in Carnoy's solution (75% methanol, 25% acetic acid) for 10 min, with 3 changes in fixation. For spreading, cells in Carnoy's solution were dropped onto glass slides and dried at 37˚C. The slides were stained with 4% Giemsa (Merck, Nottingham, UK) in phosphate buffer at pH 6.8 for 7 min, washed briefly in deionised water and air dried. The chromosome spreads were viewed on a Nikon inverted microscope (TE3000; Tokyo, Japan), using a 100x objective (Plan Apochromat, NA 1.4) and the images were captured using an Orca ER charge-coupled device camera (Hamamatsu Photonics, Bridgewater, NJ, USA). The images were processed using Photoshop (Adobe Systems Inc., CA, USA). When the images were quantified ~100 chromosome spreads were analysed.

Statistical analysis. The DNA and protein band intensity was quantified by densitometry using the BioDocAnalyze software (Biometra, Göttingen, Germany). The DNA bands were normalised with respect to the combined expression of GAPDH and ß-actin and the protein expression was normalised to the respective γ-tubulin expression. Box-plots were generated and statistical analysis was performed using GraphPad Prism 4 Software (GraphPad Software Inc., San Diego, CA, USA). Statistical significance was defined by two-tailed t-tests and analysis of variance (ANOVA). A value of

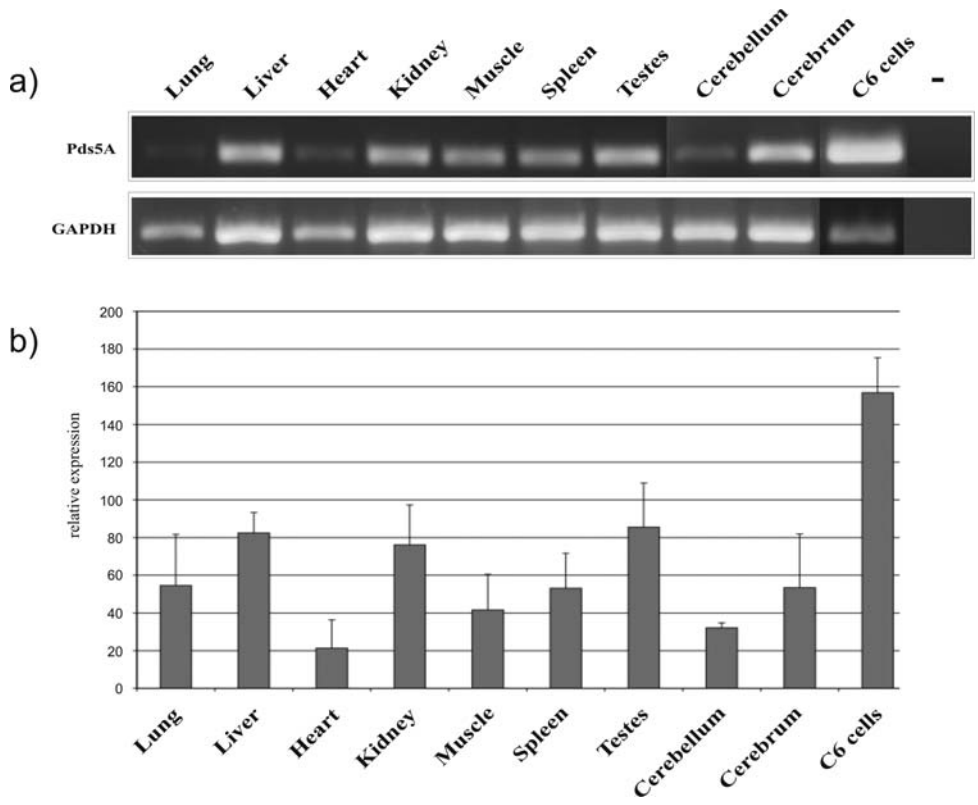

Figure 1. Expression analysis of Pds5A mRNA in 9 rat organs and C6 GBM cells. (a) Total RNA from the organs indicated and from a C6 rat glioblastoma cell line was used as the template for semiquantitative RT-PCR analysis. Primers, specific for Pds5A, were designed in flanking exons. For the negative control cDNA was excluded from the PCR reaction (-). The various cDNA concentrations were normalized to that of the housekeeping gene GAPDH, which was used as the internal loading control. The result shown is from the organs of a representative animal out of 3 animals analysed. (b) Comparison of densitometrically quantified Pds5A mRNA expression. Each value was normalised to the respective GAPDH mRNA. Shown is the median ± SD of organs from 3 animals.

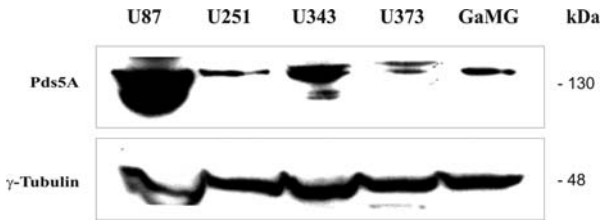

Figure 2. Western blot analysis of Pds5A protein expression by human glioblastoma cell lines. Protein lysates were isolated from U87, U251, U343, U373 and GaMG human glioblastoma cells and separated by polyacrylamide gel electrophoresis. The expressed Pds5A protein was visualized using a polyclonal Pds5A antibody. γ-tubulin served as the loading control.

$p<0.05$ was considered to be significant. All functional assays were analysed using the software R 2.9.2 (The R Foundation for Statistical Computing), including the package Rcmdr. Statistical methods used were ANOVA, linear modelling, generalised linear modelling and two-tailed t-tests. A value of $\alpha<0.05$ was considered to be significant.

Results

Cloning of Pds5A cDNA from Rattus norvegicus and its expression pattern in rat tissue. Even though the human Pds5A sequence had been published (24,25,29), only a predicted 3621 bp sequence of the rat homologue was available from the NCBI GenBank (XM_223406). Based on this sequence, we started cloning of the full-length cDNA sequence of Pds5A from the rat pheochromocytoma cell line, PC12. In contrast to the predicted sequence we found an extended coding region as a result of a shift in the boundary between exons 30 and 31. This shift causes a frameshift mutation, removing the originally predicted stop codon in exon 31. Therefore, Pds5A from *Rattus norvegicus* consists of 31 exons and comprises of 4001 bp (including start and stop codons). The full-length coding sequence has been deposited at NCBI GenBank (EF460313). Table I summarises the information and protein sequence identities for *S. cerevisiae* Pds5p, *Schizosaccharomyces pombe* Pds5$^+$, *Aspergillus nidulans* BimD, *Sordaria macrospora* Spo76, *Drosophila melanogaster* Pds5, *Caenorhabditis elegans* Evl-14, *Rattus norvegicus* Pds5A and *Homo sapiens* Pds5A and Pds5B (APRIN). The proteins are highly conserved during evolution and share a high degree of amino acid identity in a range from 19% between the budding yeast, Pds5p, to 97% for Pds5A from the rat, when compared to the human Pds5A (Table I).

In order to determine the mRNA expression pattern of Pds5A, we screened several different organs from Sprague-Dawley rats by semiquantitative RT-PCR (Fig. 1). Pds5A was expressed by all the organs tested (Fig. 1a). Whereas the heart, skeletal muscle and cerebellum displayed low mRNA

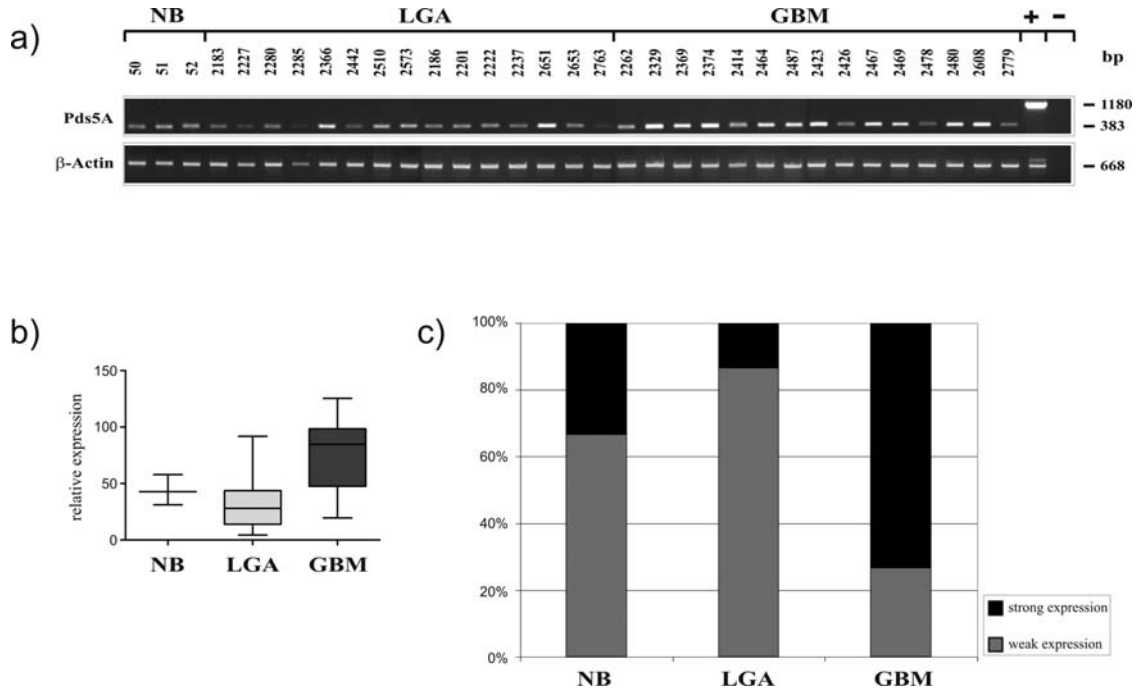

Figure 3. Expression analysis of Pds5A in NB and human astrocytic tumor samples by semiquantitative RT-PCR. (a) Total RNA from NB, LGA and GBM tissue samples was used as the template for RT-PCR analysis. Primers, specific for Pds5A, were designed in flanking exons. Genomic DNA from HBMEC cells was used as the positive control (+). For the negative control, cDNA was excluded from the PCR reaction (-). The various cDNA concentrations were normalised to that of the housekeeping gene, ß-actin, which was used as the internal loading control. The size (bp) of the cDNAs is indicated on the right. The numbers refer to the tumor samples used (50). (b) Box-plot analysis of densitometrically quantified Pds5A mRNA expression. The black line within the boxes represents the median expression, boxes show the quartiles and bars indicate minimum and maximum values. ANOVA analysis revealed a statistically significant increase of mRNA expression (p=0.0009). (c) Percentage of tissue samples expressing Pds5A mRNA. Light grey represents samples with weak expression of Pds5A mRNA [>0 but <50 on a scale from 0 (no expression detectable) to 100 (strongest expression of Pds5A, tumor 2329)] and black shows strong expression (≥50).

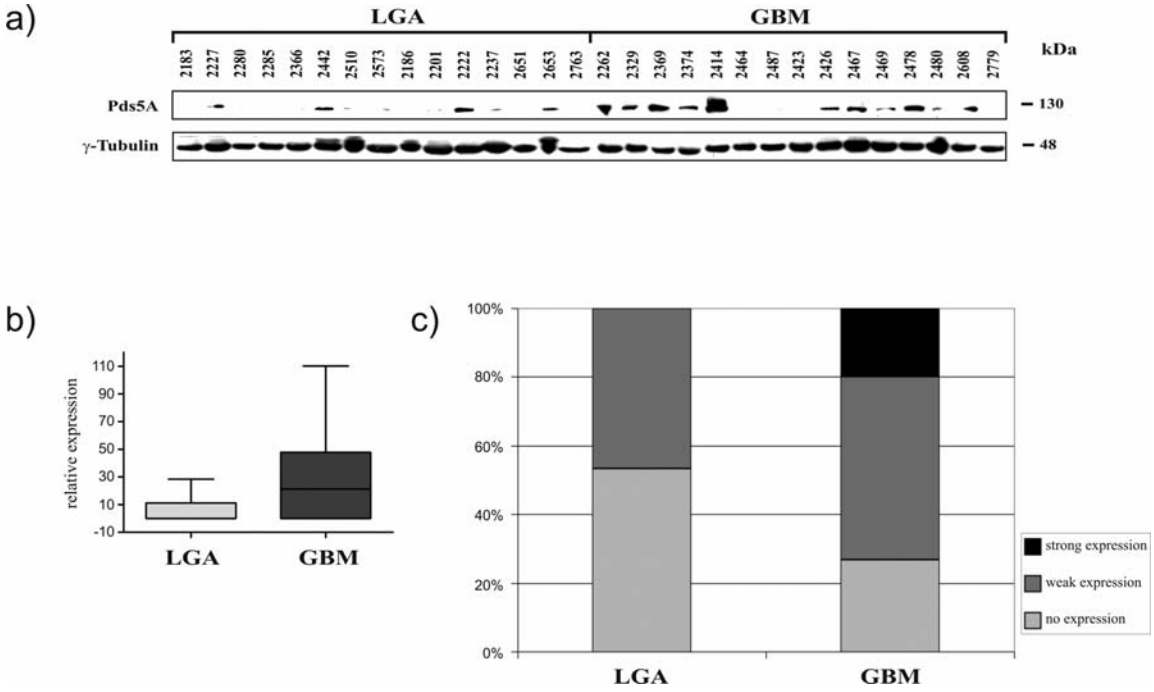

Figure 4. Western blot analysis of Pds5A protein expression in human astrocytic tumor samples. (a) Protein lysates were isolated from LGA and GBM tissue samples and separated by polyacrylamide gel electrophoresis. The expressed Pds5A protein was visualized using a polyclonal SCC-112 antibody. The numbers refer to the tumor samples used (50). γ-tubulin served as the loading control. (b) Box-plot analysis of densitometrically quantified Pds5A protein expression. The mean Pds5A expression strengths displayed by LGA and GBM had a statistically significant difference, as determined by a two-tailed t-test (p=0.0116). (c) Percentage of tissue samples expressing Pds5A protein. Light grey columns represent samples with no detectable amounts of protein, grey show weak expression [>0 but <50 on a scale from 0 (no expression detectable) to 100 (strongest expression of γ-tubulin, tumor 2467)] and black columns represent strong expression (≥50).

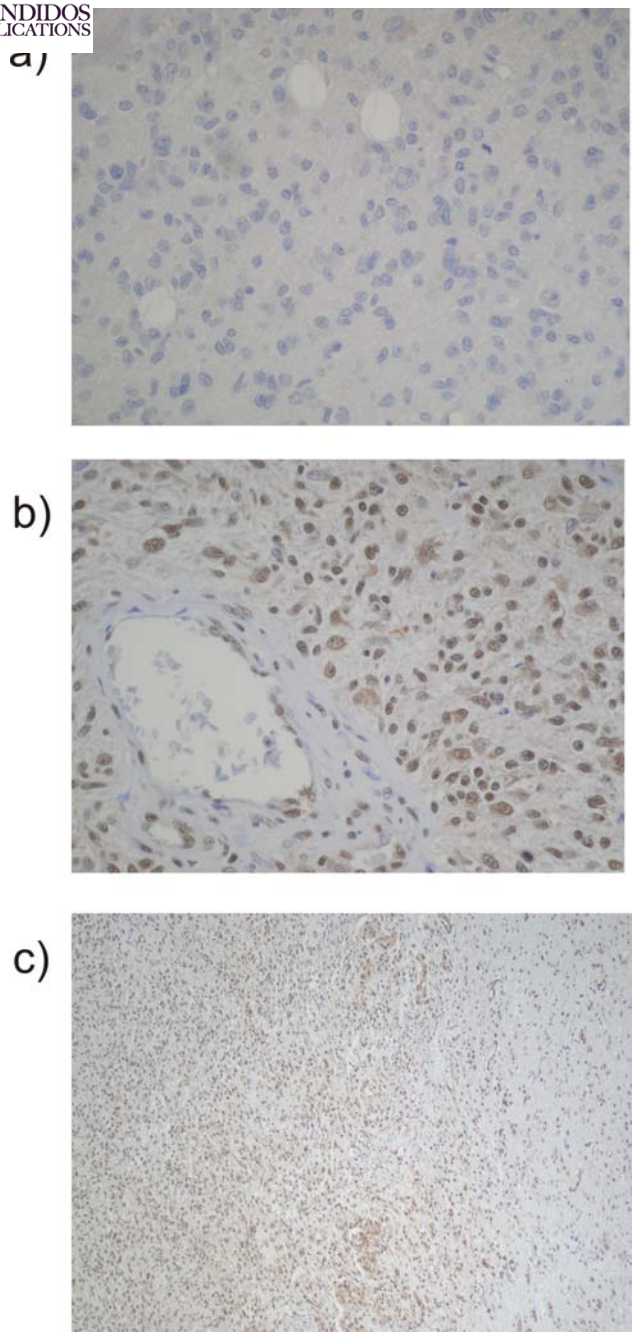

Figure 5. Pds5A expression in paraffin-embedded sections of a representative glioblastoma sample. (a-c) Pds5A expression (brown signal) was visualized by staining with a specific antibody. (a) Tissue stained with appropriate isotype control antibodies served as the negative control. Magnification, 40x (b) Nuclear staining of ~80% tumor cells. Endothelial cells around blood vessels are not stained. Magnification, 40x (c) Overview of tumor section. Left, tumor tissue; right, invasion zone. Staining of Pds5A concentrates in tumor tissue. Magnification 10x.

expression levels, the lung, spleen and cerebrum showed medium expression and the liver, kidney and testes displayed the highest levels of Pds5A mRNA (Fig. 1b). Rat C6 GBM cells, however, had a highly increased Pds5A mRNA expression in comparison to the normal rat organs (Fig. 1).

Pds5A mRNA and protein expressions are up-regulated in human high grade glioma. The high level of expression of Pds5A mRNA by rat C6 GBM cells led us to determine whether Pds5A protein could be detected in human GBM cell lines. Our Western blot analysis indicates that the Pds5A protein shows strong expression in U87 cells, medium expression in U343 cells and is weakly but clearly expressed in U251, U373 and GaMG cells (Fig. 2).

To date, human astrocytic tumors have not been analysed for the expression of Pds5A mRNA or protein. Therefore, we screened a panel of 3 NB, 15 LGA and 15 GBM surgical tissue specimens for the expression of both Pds5A mRNA (Fig. 3) and protein (Fig. 4). Pds5A mRNA was detectable in all the samples analysed (Fig. 3a). However, densitometric quantification revealed a statistically significant increase in relative expression strength (ANOVA, p=0.0009) from NB to LGA to GBM (Fig. 3b). In addition, the number of tumors with strong Pds5A mRNA expression also rose (Fig. 3c). We defined the expression strength on a scale from 0 to 100 (zero meaning no expression detectable, 100 representing the strongest Pds5A expression, which was displayed by tumor 2329). Whereas 67% of the NB samples displayed weak expression, 87% of all the GBM samples showed strong Pds5A mRNA expression (weak expression >0 but <50 on our scale and strong expression ≥50) (Fig. 3c). These results were confirmed by Western blotting of the Pds5A protein (Fig. 4). The same tissue samples that were used for RT-PCR analysis were also used for immunoblotting. The relative expression strength was significantly higher in GBM compared to LGA (two-tailed t-test, p=0.0116) (Fig. 4b). There was a high diversity in expression strength between the different glioma samples (Fig. 4a). Whereas there was no Pds5A protein detectable in half of the LGA samples (53%), 73% of the GBM samples exhibited weak (53%) to strong (20%) expression of this protein (Fig. 4c).

Pds5A was expressed in the nuclei of tumor cells in paraffin-embedded GBM sections. We performed immunohistochemistry using paraffin-embedded tissue sections derived from a number of different GBMs. A representative example is shown in Fig. 5. Tissue incubated with appropriate isotype control antibodies served as the negative control (Fig. 5a). Pds5A is a nuclear protein, expressed by ~80% of tumor cells (Fig. 5b). Some macrophages also showed cytoplasmic staining. There was no association with necrosis (data not shown) and endothelial cells were negative for Pds5A expression (Fig. 5b). Its expression was concentrated in dense tumor tissue, but was much weaker in the invasion zone (Fig. 5c).

Pds5A knockdown does not influence mitotic checkpoint function, proliferation and survival of GBM cells. The data described above indicate that Pds5A plays a role during glioma progression. Therefore, we designed siRNA for specific Pds5A protein knockdown. Transfection of 2 μM siRNA resulted in a markedly reduced Pds5A protein concentration 24 h later. The Pds5A protein concentration constantly remained at a low level for at least 144 h (Fig. 6a).

RNA interference was then used to investigate mitotic checkpoint function in U251 cells by FACS analysis (Fig. 6b). Twenty-four hours after siRNA transfection, nocodazole (25 ng/ml) was added to the cells to interfere with spindle

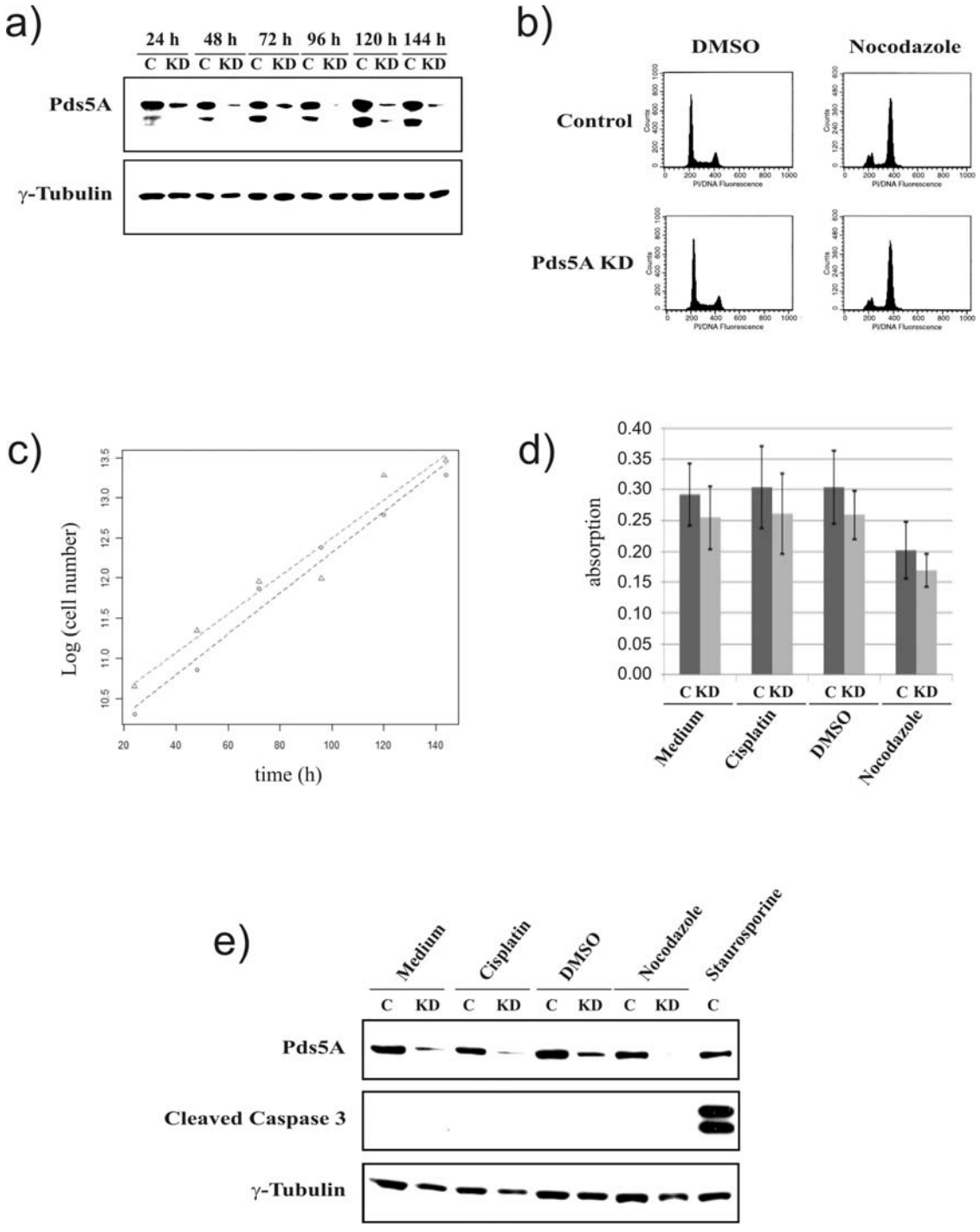

Figure 6. Pds5A knockdown does not influence the mitotic checkpoint function, proliferation and the survival of GBM cells. (a) U251 cells were transfected with 2 μM siRNA directed against Pds5A. The Pds5A knockdown was visualized by Western blotting. It remained constant over a time-period of at least 144 h. (b) FACS analysis of DMSO- (left) and nocodazole-treated (right) U251 cells, which were transfected with scrambled siRNA (control, upper panel) or were depleted of Pds5A protein by transfection with 2 μM siRNA (lower panel). Shown is 1 representative experiment out of 3. (c) Proliferation assay of U251 control (triangles) and U251 cells transfected with 750 nM siRNA directed against Pds5A (circles). Shown is the regression line of the common logarithm of cell number to time in hours and the corresponding data points for the control and knockdown cells. There was no statistically significant difference in the slope of the 2 lines. (d) MTT assay to assess the viability of U251 cells treated with or without 50 μM cisplatin for DNA damage induction and 100 ng/ml nocodazole for mitotic spindle checkpoint induction, respectively, for 24 h, each (n=4). (e) Analysis of the induction of apoptosis by Western blot and the detection of cleaved caspase-3 in GaMG cells treated for 24 h with 50 μM cisplatin and 100 ng/ml nocodazole. Staurosporine (1 μg/ml) was used as the positive control. Neither normal Pds5A protein expression (control), nor siRNA-mediated Pds5A depletion (knockdown) resulted in the induction of apoptosis under these treatment conditions. Shown is 1 representative experiment out of 3. C, control; KD, knockdown.

formation. Whereas the control, the DMSO-treated cells, showed a normal cell cycle profile, the nocodazole-treated cells were arrested in the G2/M phase of the cell cycle, as indicated by the accumulation of 4N cells and the reduction of the 2N peak in the FACS histograms (Fig. 6b). The depletion of Pds5A did not affect the function of the mitotic cell cycle checkpoint, as these cells showed the same FACS profiles as the control cells (Fig. 6b).

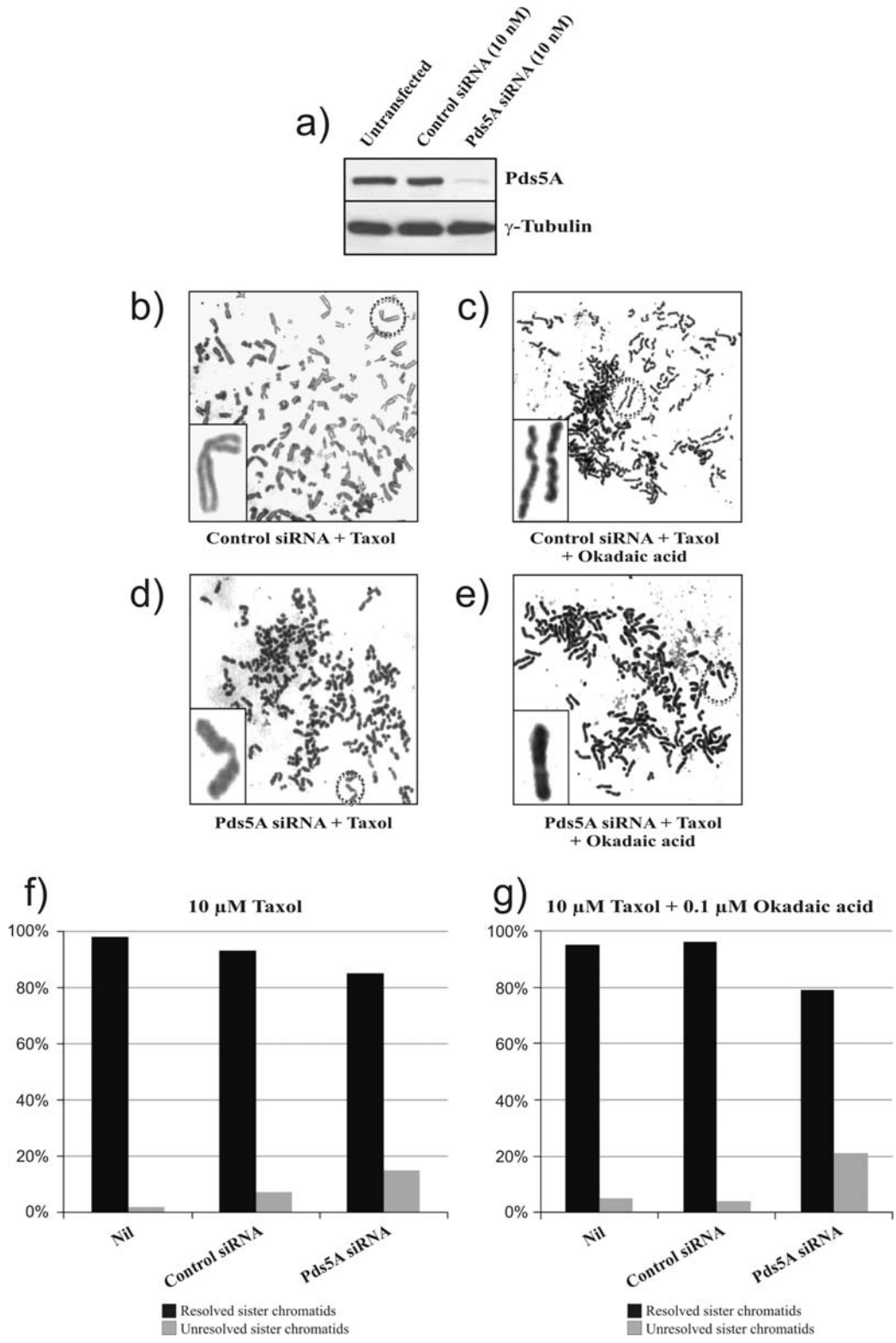

Figure 7. Pds5A is required for the resolution of sister chromatids. (a) U251 cells were transfected with either the control or a SMARTpool of Pds5A siRNAs and 48 h later the cell extracts were analysed by immunoblotting. (b-e) U251 cells were transfected with either the control or Pds5A siRNAs. Forty-eight hours later the cells were treated with either taxol (for 24 h) or taxol and okadaic acid (for 12 h). The mitotic cells were collected by shake-off and chromosome spreads were prepared by hypotonic swelling and Giemsa staining. Representative chromosomes were selected (circled) to highlight the differences in morphology observed and the enlarged images are shown in the insets. Scale bar, 20 μm. (f-g) Quantification of the chromosome spreads obtained in (b-e) and classified according to their morphology (n=100). Data from 1 representative experiment out of 2 is shown.

Also, the Pds5A knockdown did not influence cell proliferation rates (Fig. 6c). Both U251 cells expressing normal levels of Pds5A protein, and cells depleted of Pds5A, exhibited the same growth rates (Fig. 6c).

An MTT assay was used to measure the metabolic rate and thereby the viability of U251 cells. The arithmetic mean of absorbance at 570 nm for the control medium was 0.27±0.090 (Fig. 6d). Pds5A protein knockdown reduced this

value to 0.23±0.064. However, this reduction was not statistically significant (lm, p=0.24). In addition, the treatment of U251 cells with 50 μM cisplatin (a DNA-damaging agent), had no effect either in the presence or absence of Pds5A protein expression. On average, the absorbance was 100±7.6% of the control medium. In contrast, the treatment of GBM cells with 100 ng/ml nocodazole caused a significant reduction in absorbance to 73±11% of the DMSO control (lm, p=0.016). However, this was a general nocodazole effect and Pds5A expression did not significantly influence the viability of the cells (Fig. 6d).

Finally, we ascertained whether the Pds5A knockdown induced apoptosis in GBM (GaMG) cells. siRNA-transfected cells were incubated for 72 h with medium and then for another 24 h with 100 ng/ml nocodazole for the induction of the spindle checkpoint and 50 μM cisplatin for DNA-damage induction, respectively. The cells were then analysed for the presence of cleaved caspase-3 by Western blotting (Fig. 6e). The treatment of cells with staurosporine (1 μg/ml for 24 h) induced apoptosis as was assessed by cleaved caspase-3. However, the treatment of the control cells or the Pds5A-depleted cells with either cisplatin or nocodazole did not induce apoptotic cell death in GaMG or U251 cells (data not shown). In all the experiments, the successful depletion of Pds5A was analysed by Western blotting (data not shown).

Pds5A is required for resolution of sister chromatids. In order to determine whether Pds5A regulates sister chromatid cohesion, we transfected U251 cells with Pds5A siRNA, which resulted in the efficient depletion of the Pds5A protein (Fig. 7a). The siRNA-treated cells were arrested during mitosis either by treatment with taxol alone or with a combination of taxol and okadaic acid. The mitotically-arrested cells were collected by shake-off and their chromosomes were analysed by spreading and Giemsa staining. Chromosome spreads prepared from taxol-treated, control siRNA-transfected cells displayed the expected X-shaped morphology with resolved sister chromatid arms but were still attached to the centromere (Fig. 7b) (55). However, chromosomes from Pds5A-depleted cells displayed a different morphology (Fig. 7d). Fifteen percent of the chromosome spreads prepared from Pds5A-depleted cells displayed unresolved sister chromatid arms compared to 7% in the control siRNA-treated cells (Fig. 7f). Furthermore, in order to determine whether Pds5A was also required for sister chromatid resolution at the centromere, we treated siRNA-transfected cells with a combination of taxol and okadaic acid (an inhibitor of protein phosphatase type 2A). As expected, in the control siRNA cells, 96% of the chromosomes displayed the complete separation of sister chromatids at both the arms and the centromere (Fig. 7c and g) whereas in the absence of Pds5A, only 79% of the spreads examined displayed complete separation of sisters (Fig. 7e and g). This result suggests that Pds5A is required for sister chromatid separation at both the arms and centromere during mitosis.

Discussion

Pds5A is a cohesin complex-interacting protein, which is involved in the establishment, maintenance and dissolution of sister chromatid cohesion (27-30,34,35). Although details about its function remain unresolved, it could also play a role in tumorigenesis (25,26).

Here, we describe the cloning of Pds5A from *Rattus norvegicus* and analyse its expression pattern in rat tissue (Fig. 1). As our initial analysis indicated that levels of Pds5A mRNA were highly elevated in C6 rat GBM cells, we analysed the expression of Pds5A protein in human GBM cell lines by Western blotting (Fig. 2). The high level of expression of Pds5A in human GBM cell lines led us to determine both the Pds5A mRNA and protein expression in patient biopsies of LGA and GBM (Figs. 3 and 4). We found a statistically significant increase in both the Pds5A mRNA and protein levels that correlated positively with the WHO grade of the tumor. Finally, in the paraffin-embedded tissue sections, we observed a high level of nuclear expression of Pds5A in dense tumor tissue and a much weaker expression within the invasion zone (Fig. 5). Our data indicate that Pds5A does not play a role in mitotic checkpoint function and cell proliferation or survival in U251 GBM cells, either with or without the induction of spindle and DNA damage, respectively (Fig. 6). However, our results suggest that Pds5A could regulate sister chromatid cohesion in these cells (Fig. 7).

When we started the cloning of Pds5A, knowledge about its gene structure in *Rattus norvegicus* was based on *in silico* methods and sequence comparisons designed to detect homologies between different species. Therefore, there was only a predicted 3621 bp sequence (GenBank: XM_223406). Our analysis revealed a shift in the boundary between exons 30 and 31, leading to a frameshift and the removal of the originally predicted stop codon in exon 31, thereby extending the coding region of Pds5A to 4001 bp (1333 amino acids). The GenBank sequence, which was updated in the meantime, now confirms our results. As our *Rattus norvegicus* Pds5A cDNA data were based on experimental approaches, the sequence was deposited at NCBI GenBank (EF460313). At the protein level, Pds5A shares 97% identity with its human ortholog, 86% with the *Xenopus laevis* Pds5A and 19% with its ortholog Pds5p from *S. cerevisiae* (Table I). It has been reported that the human Pds5A shows 23% identity with the *S. cerevisiae* Pds5p (25). However, the sequence reported by Kumar *et al* (25) lacked several residues at its N-terminus (29) and this could explain why we found only 19% identity between the human and budding yeast protein sequences (Table I). In accordance with previous reports, we found 23% identity between human Pds5A and *Aspergillus nidulans* BimD proteins (40).

The involvement of Pds5A in mitosis (23-26) implies a broad expression in body tissues. Indeed, we found the highest expression of Pds5A mRNA in the liver, kidney and testes, all the organs with high rates of cell division, whereas the lung, spleen and cerebrum displayed medium expression. The heart, skeletal muscle and cerebellum had low Pds5A mRNA expression (Fig. 1). In adult mice, high expression of Pds5A mRNA has been reported in the thymus, testis, spleen and lung (36), whereas the brain and kidney displayed intermediate expression and the heart, liver, prostate and stomach, low expression (36). Also, in human organs, Pds5A expression was very broad and is consistent with our data

he protein level, Pds5A has been shown to be present ıg, breast, ovary, kidney and strong expression has been observed in colon tissue (25). As we found strong Pds5A mRNA expression in rat C6 glioblastoma cells, we screened diverse human GBM cell lines for Pds5A protein expression by Western blotting (Fig. 2) and found strong expression in U87, medium expression in U343 and weak, but clearly detectable expression in the other cell lines tested (Fig. 2). This is the first analysis of Pds5A expression in human malignant astrocytomas. However, diverse breast and nasopharyngeal epithelial cancer cell lines have been analysed and these have also been shown to express high protein levels of Pds5A during the G2/M phase of the cell cycle (25,26). In both breast and kidney tumor samples, Pds5A mRNA has been shown to be down-regulated in comparison to the corresponding normal tissues (25), but in tumors of the oesophagus, stomach, liver and colon, Pds5A mRNA and protein levels were increased (26). In our analysis, Pds5A expression was significantly increased at both the mRNA and protein level, and this increase correlated with the WHO grading of the human gliomas (Figs. 3 and 4). The paraffin-embedded tissue sections displayed the strongest Pds5A expression within the dense tumor tissue in 80% of tumor cells (Fig. 5). This overexpression was not associated with dividing cells as determined by Ki67 staining (data not shown). Therefore, our data suggest that Pds5A could have additional functions during tumorigenesis, besides promoting proliferation.

Therefore, we analysed whether the Pds5A protein knockdown by RNA interference could have any influence on mitotic checkpoint response, proliferation rate or the survival of GBM cells. In a global transcriptional analysis of budding yeast expressing mutated Pds5p, 6 genes involved in the mitotic checkpoint were up-regulated (56). For this reason, our Pds5A knockdown was combined with nocodazole for the obstruction of spindle formation. However, mitotic spindle checkpoint function remained normal (Fig. 6b).

An aspect of GBM is the association of the promoter methylation status of the O^6-methylguanine DNA methyltransferase (*MGMT*) gene with tumor response to chemotherapies (57). *MGMT* codes for O^6-alkylguanine DNA alkyltransferase (AGT), a DNA repair enzyme that removes alkyl adducts (57,58). Therefore, its down-regulation is negatively associated with the capability of GBM cells to repair DNA defects introduced by chemotherapeutics (57,58). Temozolomide for example, the standard drug used in combination with γ-irradiation for the treatment of GBM (48), is a DNA alkylating agent (59). Frequently, such DNA alterations are mutagenic or lead to DNA strand breaks and subsequently to apoptosis (58). A functional AGT is able to repair such defects and thereby allows for the survival of affected cells (58). It has been shown that BimD, Spo76, $Pds5^+$ and Pds5p mutants are hypersensitive after exposure to DNA damaging agents (39-41,60), suggesting that the human Pds5A could possibly play a similar role in DNA repair. Therefore, we also included the treatment of GBM cells with cisplatin for the induction of DNA damage in our experiments. Nevertheless, Pds5A depleted cells did not develop hypersensitivity to the cisplatin-induced DNA damage (Fig. 6d and e).

The mutation of *S. cerevisiae* Pds5p causes cell death with features characteristic of apoptosis such as the accumulation of DNA breaks, the condensation and fragmentation of chromatin, the fragmentation of nuclei and cell size enlargement (56,60). In vertebrate cells, Pds5A overexpression causes either an increase in apoptosis (25) or an enhancement of malignant cell behavior (26), depending on the cell line used. In our experiments, however, we did not see such effects. The proliferation rate did not change (Fig. 6c) and there was neither a decrease in the viability of GBM cells (Fig. 6d) nor an increase in apoptosis 24 h after treatment with nocodazole or cisplatin (Fig. 6e).

The human Pds5B protein, a paralog of Pds5A, originally isolated as androgene shutoff gene 3 (AS3) from LNCaP prostate cancer cell lines (61) and later designated as APRIN, is a chromatin regulator in hormonal differentiation (62). It shares 73% amino acid identity with Pds5A (Table I) and has been shown to be involved in the regulation of proliferative arrest in cancer cells in response to hormones (61,62). It is a putative tumor suppressor (63,64). It has also been reported that Pds5B can functionally compensate for Pds5A loss (36,65). Therefore, the lack of the above-mentioned effects in our knockdown experiments could be due to the activity of Pds5B in these cells.

Our data in this study support earlier observations that Pds5A plays a key role in releasing cohesin from chromosomes and in sister chromatid segregation (Fig. 7) (42,65,66), although the exact mechanism remains unclear. Pds5A could also function during embryonic development (36,67) and tumorigenesis (25,26). In addition, signalling pathways could have some influence on the regulation of Pds5 protein family members. Bioinformatic studies have revealed that Pds5A contains binding domains for Ras, Rho, RhoGEF, phosphatidyinositol-3 kinase and cyclin (26), suggesting putative regulation by mitogenic signalling pathways. There is evidence that the mitogenic MAPK cascade is functionally important for glioma proliferation (53,68-71). However, whether there is a direct link between mitogenic signalling and the regulation of Pds5A, has not yet been elucidated. Our ongoing research is addressing this question in conjunction with Pds5B function in GBM cells.

In summary, our data show that Pds5A is up-regulated in GBM, correlating with the WHO grade of human malignant glioma. Although studies have suggested a possible role of Pds5A in mitotic cell division control, mitogenic signalling, apoptosis and DNA repair processes, we only observed an effect of Pds5A on sister chromatid cohesion. Nevertheless, Pds5A, in conjunction with Pds5B, which is able to substitute for its loss (36,65), could turn out to be a promising new target to prevent the progression of LGAs to high grade malignancies and to advance our current treatment options for GBM in the future.

Acknowledgements

We thank Thomas Freiman (Neurochirurgische Klinik, Neurozentrum, University Hospital of Freiburg im Breisgau, Germany) for the NB control tissue and Michaela Kapp (University of Würzburg, Department of Gynaecology and Obstetrics, Würzburg, Germany) for technical assistance.

References

1. Dey P: Aneuploidy and malignancy: an unsolved equation. J Clin Pathol 57: 1245-1249, 2004.
2. Rajagopalan H and Lengauer C: Aneuploidy and Cancer. Nature 432: 338-341, 2004.
3. Von Deinling A, Louis DN and Wiestler OD: Molecular pathways in the formation of gliomas. Glia 15: 328-338, 1995.
4. Cahill DP, Kinzler KW, Vogelstein B and Lengauer C: Genetic instability and darwinian selection in tumours. Trends Cell Biol 9: M57-M60, 1999.
5. Shapiro JR: Genetic alterations associated with adult diffuse astrocytic tumors. Am J Med Genet 115: 194-201, 2002.
6. Duesberg P, Li R, Fabarius A and Hehlmann R: The chromosomal basis of cancer. Cell Oncol 27: 293-318, 2005.
7. Gao CF, Furge K, Koeman J, Dykema K, Cutler ML, Werts A, Haak P and Vande Woude GF: Chromosome instability, chromosome transcriptome, and clonal evolution of tumor cell populations. Proc Natl Acad Sci USA 104: 8995-9000, 2007.
8. Lopes CS and Sunkel CE: The spindle checkpoint: From normal cell division to tumorigenesis. Arch Med Res 34: 155-165, 2003.
9. Bharadwaj R and Yu H: The spindle checkpoint, aneuploidy, and cancer. Oncogene 23: 2016-2027, 2004.
10. Tanaka K, Nishioka J, Kato K, Nakamura A, Mouri T, Miki C, Kusunoki M and Nobori T: Mitotic checkpoint protein hsMAD2 as a marker predicting liver metastasis of human gastric cancers. Jpn J Cancer Res 92: 952-958, 2001.
11. Shichiri M, Yoshinaga K, Hisatomi H, Sugihara K and Hirata Y: Genetic and epigenetic inactivation of mitotic checkpoint genes hBub1 and hBubR1 and their relationship to survival. Cancer Res 62: 13-17, 2002.
12. Yuan B, Xu Y, Woo JH, Wang Y, Bae YK, Yoon DS, Wersto RP, Tully E, Wilsbach K and Gabrielson E: Increased expression of mitotic checkpoint genes in breast cancer cells with chromosomal instability. Clin Cancer Res 12: 405-410, 2006.
13. Babu JR, Jeganathan KB, Baker DJ, Wu X, Kang-Decker N and van Deursen JM: Rae1 is an essential mitotic checkpoint regulator that cooperates with Bub3 to prevent chromosome missegregation. J Cell Biol 160: 341-353, 2003.
14. Dai W, Wang Q, Liu T, Swamy M, Fang Y, Xie S, Mahmood R, Yang YM, Xu M and Rao CV: Slippage of mitotic arrest and enhanced tumor development in mice with BubR1 haploinsufficiency. Cancer Res 64: 440-445, 2004.
15. Sotillo R, Hernando E, Díaz-Rodríguez E, Teruya-Feldstein J, Cordón-Cardo, C, Lowe SW and Benezra R: Mad2 overexpression promotes aneuploidy and tumorigenesis in mice. Cancer Cell 11: 9-23, 2007.
16. Weaver BAA, Silk AD, Montagna C, Verdier-Pinard P and Cleveland DW: Aneuploidy acts both oncogenically and as a tumor suppressor. Cancer Cell 11: 25-36, 2007.
17. Matsuura S, Ito E, Tauchi H, Komatsu K, Ikeuchi T and Kajii T: Chromosomal instability syndrome of total premature chromatid separation with mosaic variegated aneuploidy is defective in mitotic-spindle checkpoint. Am J Hum Genet 67: 483-486, 2000.
18. Hanks S, Coleman K, Reid S, Plaja A, Firth H, FitzPatrick D, Kidd A, Méhes K, Nash R, Robin N, Shannon N, Tolmie J, Swansbury J, Irrthum A, Douglas J and Rahman N: Constitutional aneuploidy and cancer predisposition caused by biallelic mutations in BUB1B. Nat Genet 36: 1159-1161, 2004.
19. Hanks S, Coleman K, Summersgill B, Messahel B, Williamson D, Pritchard-Jones, K, Strefford J, Swansbury J, Plaja A, Shipley J and Rahman N: Comparative genomic hybridization and BUB1B mutation analyses in childhood cancers associated with mosaic variegated aneuploidy syndrome. Cancer Lett 239: 234-238, 2006.
20. Matsuura S, Matsumoto Y, Morishima K, Izumi H, Matsumoto H, Ito E, Tsutsui K, Kobayashi J, Tauchi H, Kajiwara Y, Hama S, Kuriso K, Tahara H, Oshimura M, Komatsu K, Ikeuchi T and Kajii T: Monoallelic BUB1B mutations and defective mitotic-spindle checkpoint in seven families with premature chromatid separation (PCS) syndrome. Am J Med Genet 140: 358-367, 2006.
21. Kajii T, Ikeuchi T, Yang ZQ, Makamura Y, Tsuji Y, Yokomori K, Kawamura M, Fukuda S, Horita S and Asamoto A: Cancer-prone syndrome of mosaic variegated aneuploidy and total premature chromatid separation: Report of five infants. Am J Med Genet 104: 57-64, 2001.
22. Plaja A, Vendrell T, Smeets D, Sarret E, Gili T, Català V, Mediano C and Scheres JM: Variegated aneuploidy related to premature centromere division (PCD) is expressed in vivo and is a cancer-prone disease. Am J Med Genet 98: 216-223, 2001.
23. Hartman T, Stead K, Koshland D and Guacci V: Pds5p is an essential chromosomal protein required for both sister chromatid cohesion and condensation in *Saccharomyces cerevisiae*. J Cell Biol 151: 613-626, 2000.
24. Sumara I, Vorlaufer E, Gieffers C, Peters BH and Peters JM: Characterization of vertebrate cohesin complexes and their regulation in prophase. J Cell Biol 151: 749-761, 2000.
25. Kumar D, Sakabe I, Patel S, Zhang Y, Ahmad I, Gehan EA, Whiteside TL and Kasid U: SCC-112, a novel cell cycle-regulated molecule, exhibits reduced expression in human renal carcinomas. Gene 328: 187-196, 2004.
26. Zheng MZ, Zheng LM and Zeng YX: SCC-112 gene is involved in tumor progression and promotes the cell proliferation in G2/M phase. J Cancer Res Clin Oncol 134: 453-462, 2008.
27. Panizza S, Tanaka T, Hochwagen, A, Eisenhaber F and Nasmyth K: Pds5 cooperates with cohesin in maintaining sister chromatid cohesion. Curr Biol 10: 1557-1564, 2000.
28. Wang F, Yoder J, Antoshechkin I and Han M: *Caenorhabditis elegans* EVL-14/PDS-5 and SCC-3 are essential for sister chromatid cohesion in meiosis and mitosis. Mol Cell Biol 23: 7698-7707, 2003.
29. Losada A, Yokochi T and Hirano T: Functional contribution of Pds5 to cohesin-mediated cohesion in human cells and *Xenopus* egg extracts. J Cell Sci 118: 2133-2141, 2005.
30. Guacci V: Sister chromatid cohesion: the cohesin cleavage model does not ring true. Genes Cells 12: 693-708, 2007.
31. Yu H: Regulation of APC-Cdc20 by the spindle checkpoint. Curr Opin Cell Biol 14: 706-714, 2002.
32. Nasmyth K and Haering CH: The structure and function of SMC and kleisin complexes. Annu Rev Biochem 74: 595-648, 2005.
33. Uhlmann F: What is your assay for sister-chromatid cohesion? EMBO J 26: 4609-4618, 2007.
34. Tanaka K, Hao Z, Kai M and Okayama H: Establishment and maintenance of sister chromatid cohesion in fission yeast by a unique mechanism. EMBO J 20: 5779-5790, 2001.
35. Stead K, Aguilar C, Hartman T, Drexel M, Meluh P and Guacci V: Pds5p regulates the maintenance of sister chromatid cohesion and is sumoylated to promote the dissolution of cohesion. J Cell Biol 163: 729-741, 2003.
36. Zhang B, Chang J, Fu M, Huang J, Kashyap R, Salavaggione E, Jain S, Kulkarni S, Deardorff MA, Uziella ML, Dorsett D, Beebe DC, Jay PY, Heuckeroth RO, Krantz I and Milbrandt J: Dosage effects of cohesin regulatory factor PDS5 on mammalian development: Implications for cohesinopathies. PloS One 4: e5232, 2009.
37. Kadyk LC and Hartwell LH: Sister chromatids are preferred over homologs as substrates for recombinational repair in *Saccharomyces cerevisiae*. Genetics 132: 387-402, 1992.
38. Jin H, Guacci V and Yu H-G: Pds5 is required for homologue pairing and inhibits synapsis of sister chromatids during yeast miosis. J Cell Biol 186: 713-725, 2008.
39. Moreau PJF, Zickler D and Leblon G: One class of mutants with disturbed centromere cleavage and chromosome pairing in *Sordaria macrospora*. Mol Gen Genet 198: 189-197, 1985.
40. Denison SH, Kafer E and May GS: Mutation in the bimD gene of *Aspergillus nidulans* confers a conditional mitotic block and sensitivity to DNA damaging agents. Genetics 134: 1085-1096, 1993.
41. Wang SW, Read RL and Norbury CJ: Fission yeast Pds5 is required for accurate chromosome segregation and for survival after DNA damage or metaphase arrest. J Cell Sci 115: 587-598, 2002.
42. Terret M-E, Sherwood R, Rahman S, Qin J and Jallepalli PV: Cohesin acetylation speeds the replication fork. Nature 462: 231-235, 2009.
43. Heller RC and Marians KJ: Replisome assembly and the direct restart of stalled replication forks. Nat Rev Mol Cell Biol 7: 932-943, 2006.
44. Cianculli AM, Morace E, Coletta AM, Occhipinti E, Gandolfo GM, Leorardo G and Carapella CM: Investigation of genetic alterations associated with development and adverse outcome in patients with astrocytic tumor. J Neurooncol 48: 95-101, 2000.
45. Loeper S, Romeike BFM, Heckmann N, Jung V, Henn W, Feiden W, Zhang KD and Urbschat S: Frequent mitotic errors in tumor cells of genetically micro-heterogeneous glioblastomas. Cytogenet Cell Genet 94: 1-8, 2001.

47. Cavenee WK, Furnari FB, Nagane M, Huang H-JS, Newcomb EW, Bigner DD, Weller M, Berens ME, Plate KH, Israel MA, Noble MD and Kleihues P: Diffusely infiltrating astrocytomas. In: Pathology and Genetics of Tumors of the Nervous System. WHO Classification of Tumors. Kleihues P and Cavenee WK (eds). IARC Press, Lyon, pp10-21, 2000.
48. Stupp R, Mason WP, van den Bent MJ, Weller M, Fisher B, Taphoorn MJ, Belanger K, Brandes AA, Marosi C, Bogdahn U, Curschmann J, Janzer RC, Ludwin SK, Gorlia T, Allgeier A, Lacombe D, Cairncross JG, Eisenhauer E, Mirimanoff RO; European Organisation for Research and Treatment of Cancer Brain Tumor and Radiotherapy Groups; National Cancer Institute of Canada Clinical Trials Group: Radiotherapy plus concomitant and adjuvant temozolomide for glioblastoma. N Engl J Med 352: 987-996, 2005.
49. Kleihues P, Louis DN, Scheithauer BW, Rorke LB, Reifenberger G, Burger PC and Cavenee WK: The WHO classification of tumors of the nervous system. J Neuropathol Exp Neurol 61: 215-225, 2002.
50. Stojic J, Hagemann C, Haas S, Herbold C, Kühnel S, Gerngras S, Roggendorf W, Roosen K and Vince GH: Expression of matrix metalloproteinases MMP-1, MMP-11 and MMP-19 is correlated with the WHO-grading of human malignant gliomas. Neurosci Res 60: 40-49, 2008.
51. Akslen LA, Andersen KJ and Bjerkvig R: Characteristics of human and rat glioma cells grown in a defined medium. Anticancer Res 8: 797-803, 1988.
52. Hagemann C, Meyer C, Stojic J, Eicker S, Gerngras S, Kühnel S, Roosen K and Vince GH: High efficiency transfection of glioma cell lines and primary cells for overexpression and RNAi experiments. J Neurosci Methods 156: 194-202, 2006.
53. Hagemann C, Gloger J, Anacker J, Said HM, Gerngras S, Kühnel S, Meyer C, Rapp UR, Kämmerer U, Vordermark D, Flentje M, Roosen K and Vince GH: RAF expression in human astrocytic tumors. Int J Mol Med 23: 17-31, 2009.
54. Hagemann C, Anacker J, Gerngras S, Kühnel S, Said HM, Patel R, Kämmerer U, Vordermark D, Roosen K and Vince GH: Expression analysis of the autosomal recessive primary microcephaly genes MCPH1 (microcephalin) and MCPH5 (ASPM, abnormal spindle like, microcephaly associated) in human malignant gliomas. Oncol Rep 20: 301-308, 2008.
55. Kitajima TS, Sakuno T, Ishiguro K, Iemura S, Natsume T, Kawashima SA and Watanabe Y: Shugoshin collaborates with protein phosphatase 2A to protect cohesin. Nature 441: 46-52, 2003.
56. Ren Q, Yang H, Gao B and Zhang Z: Global transcriptional analysis of yeast cell death induced by mutation of sister chromatid cohesin. Comp Funct Genomics 634283, 2008.
57. Ibdaih A, Omuro A, Ducray F and Hoang-Xuan K: Molecular genetic markers as predictors of response to chemotherapy in gliomas. Curr Opin Oncol 19: 606-611, 2007.
58. Gerson SL: MGMT: Its role in cancer aetiology and cancer therapeutics. Nat Rev Cancer 4: 296-307, 2004.
59. Newlands ES, Stevens MFG, Wedge SR, Wheelhouse RT and Brock C: Temozolomide: a review of its discovery, chemical properties, pre-clinical development and clinical trials. Cancer Treat Rev 23: 35-61, 1997.
60. Ren Q, Yang H, Rosinski M, Conrad MN, Dresser ME, Guacci V and Zhang Z: Mutation of the cohesin related gene PDS5 causes cell death with predominant apoptotic features in *Saccharomyces cerevisiae* during early mitosis. Mutat Res 570: 163-173, 2005.
61. Geck P, Szelei J, Jimenez J, Sonnenschein C and Soto AM: Early gene expression during androgen-induced inhibition of proliferation of prostate cancer cells: a new suppressor candidate on chromosome 13, in the BRCA2-Rb1 locus. J Steroid Biochem Mol Biol 68: 41-50, 1999.
62. Maffini M, Denes V, Sonnenschein C, Soto A and Geck P: APRIN is a unique Pds5 paralog with features of a chromatin regulator in homonal differentiation. J Steroid Biochem Mol Biol 108: 32-43, 2008.
63. Zhang Y, Huang X, Qi J, Yan C, Xu X, Han Y and Wang M: Correlation of genomic and expression alterations of AS3 with esophageal squamous cell carcinoma. J Genet Genomics 35: 267-271, 2008.
64. Denes V, Pilichowska M, Makarovskiy A, Carpinito G and Geck P: Loss of a cohesin-linked suppressor APRIN (Pds5b) disrupts stem cell programs in embryonal carcinoma: an emerging cohesin role in tumor suppression. Oncogene 29: 3446-3452, 2010.
65. Shintomi K and Hirano T: Releasing cohesin from chromosome arms in early mitosis: opposing actions of Wap1-Pds5 and Sgo1. Genes Dev 23: 2224-2236, 2009.
66. Sutani T, Kawaguchi T, Kanno R, Itoh T and Shirahige K: Budding yeast Wpl1 (Rad61)-Pds5 complex counteracts sister chromatid cohesion-establishing reaction. Curr Biol 19: 492-497, 2009.
67. Dorsett D: Cohesin, gene expression and development: Lessons from *Drosophila*. Chromosome Res 17: 185-200, 2009.
68. Holland EC, Celestino J, Dai C, Schaefer L, Sawaya RE and Fuller GN: Combined activation of Ras and Akt in neural progenitors induces glioblastoma formation in mice. Nat Genet 25: 55-57, 2000.
69. Ding H, Roncari L, Shannon P, Wu X, Lau N, Karaskova J, Gutmann DH, Squire JA, Nagy A and Guha A: Astrocyte specific expression of activated p21-ras results in malignant astrocytoma formation in a transgenic mouse model of human gliomas. Cancer Res 61: 3826-3836, 2001.
70. Edwards LA, Verreault M, Thiessen B, Dragowska, WH, Hu Y, Yeung JHF, Dedhar S and Bally MB: Combined inhibition of the phosphatidyl 3-kinase/Akt and Ras/mitogen-activated protein kinase pathways results in synergistic effects in glioblastoma cells. Mol Cancer Ther 5: 645-654, 2006.
71. Sathornsumetee S, Hjelmeland AB, Keir ST, McLendon RE, Batt D, Ramsey T, Yusuff N, Rasheed BK, Kieran MW, Laforme A, Bigner DD, Friedman HS and Rich JN: AAL881, a novel small molecule inhibitor of RAF and vascular endothelial growth factor receptor activities, blocks the growth of malignant glioma. Cancer Res 66: 8722-8730, 2006.